

Search for $Z_c(3900)^\pm \rightarrow \omega\pi^\pm$

M. Ablikim¹, M. N. Achasov^{9,f}, X. C. Ai¹, O. Albayrak⁵, M. Albrecht⁴, D. J. Ambrose⁴⁴, A. Amoroso^{48A,48C}, F. F. An¹, Q. An^{45,a}, J. Z. Bai¹, R. Baldini Ferroli^{20A}, Y. Ban³¹, D. W. Bennett¹⁹, J. V. Bennett⁵, M. Bertani^{20A}, D. Bettoni^{21A}, J. M. Bian⁴³, F. Bianchi^{48A,48C}, E. Boger^{23,d}, I. Boyko²³, R. A. Briere⁵, H. Cai⁵⁰, X. Cai^{1,a}, O. Cakir^{40A,b}, A. Calcaterra^{20A}, G. F. Cao¹, S. A. Cetin^{40B}, J. F. Chang^{1,a}, G. Chelkov^{23,d,e}, G. Chen¹, H. S. Chen¹, H. Y. Chen², J. C. Chen¹, M. L. Chen^{1,a}, S. J. Chen²⁹, X. Chen^{1,a}, X. R. Chen²⁶, Y. B. Chen^{1,a}, H. P. Cheng¹⁷, X. K. Chu³¹, G. Cibinetto^{21A}, H. L. Dai^{1,a}, J. P. Dai³⁴, A. Dbeysi¹⁴, D. Dedovich²³, Z. Y. Deng¹, A. Denig²², I. Denysenko²³, M. Destefanis^{48A,48C}, F. De Mori^{48A,48C}, Y. Ding²⁷, C. Dong³⁰, J. Dong^{1,a}, L. Y. Dong¹, M. Y. Dong^{1,a}, S. X. Du⁵², P. F. Duan¹, E. E. Eren^{40B}, J. Z. Fan³⁹, J. Fang^{1,a}, S. S. Fang¹, X. Fang^{45,a}, Y. Fang¹, L. Fava^{48B,48C}, F. Feldbauer²², G. Felici^{20A}, C. Q. Feng^{45,a}, E. Fioravanti^{21A}, M. Fritsch^{14,22}, C. D. Fu¹, Q. Gao¹, X. Y. Gao², Y. Gao³⁹, Z. Gao^{45,a}, I. Garzia^{21A}, C. Geng^{45,a}, K. Goetzen¹⁰, W. X. Gong^{1,a}, W. Gradl²², M. Greco^{48A,48C}, M. H. Gu^{1,a}, Y. T. Gu¹², Y. H. Guan¹, A. Q. Guo¹, L. B. Guo²⁸, Y. Guo¹, Y. P. Guo²², Z. Haddadi²⁵, A. Hafner²², S. Han⁵⁰, Y. L. Han¹, X. Q. Hao¹⁵, F. A. Harris⁴², K. L. He¹, Z. Y. He³⁰, T. Held⁴, Y. K. Heng^{1,a}, Z. L. Hou¹, C. Hu²⁸, H. M. Hu¹, J. F. Hu^{48A,48C}, T. Hu^{1,a}, Y. Hu¹, G. M. Huang⁶, G. S. Huang^{45,a}, H. P. Huang⁵⁰, J. S. Huang¹⁵, X. T. Huang³³, Y. Huang²⁹, T. Hussain⁴⁷, Q. Ji¹, Q. P. Ji³⁰, X. B. Ji¹, X. L. Ji^{1,a}, L. L. Jiang¹, L. W. Jiang⁵⁰, X. S. Jiang^{1,a}, X. Y. Jiang³⁰, J. B. Jiao³³, Z. Jiao¹⁷, D. P. Jin^{1,a}, S. Jin¹, T. Johansson⁴⁹, A. Julin⁴³, N. Kalantar-Nayestanaki²⁵, X. L. Kang¹, X. S. Kang³⁰, M. Kavatsyuk²⁵, B. C. Ke⁵, P. Kiese²², R. Kliemt¹⁴, B. Kloss²², O. B. Kolcu^{40B,i}, B. Kopf⁴, M. Kornicer⁴², W. Kühn²⁴, A. Kupsc⁴⁹, J. S. Lange²⁴, M. Lara¹⁹, P. Larin¹⁴, C. Leng^{48C}, C. Li⁴⁹, C. H. Li¹, Cheng Li^{45,a}, D. M. Li⁵², F. Li^{1,a}, G. Li¹, H. B. Li¹, J. C. Li¹, Jin Li³², K. Li¹³, K. Li³³, Lei Li³, P. R. Li⁴¹, T. Li³³, W. D. Li¹, W. G. Li¹, X. L. Li³³, X. M. Li¹², X. N. Li^{1,a}, X. Q. Li³⁰, Z. B. Li³⁸, H. Liang^{45,a}, Y. F. Liang³⁶, Y. T. Liang²⁴, G. R. Liao¹¹, D. X. Lin¹⁴, B. J. Liu¹, C. X. Liu¹, F. H. Liu³⁵, Fang Liu¹, Feng Liu⁶, H. B. Liu¹², H. H. Liu¹⁶, H. H. Liu¹, H. M. Liu¹, J. Liu¹, J. B. Liu^{45,a}, J. P. Liu⁵⁰, J. Y. Liu¹, K. Liu³⁹, K. Y. Liu²⁷, L. D. Liu³¹, P. L. Liu^{1,a}, Q. Liu⁴¹, S. B. Liu^{45,a}, X. X. Liu²⁶, X. X. Liu⁴¹, Y. B. Liu³⁰, Z. A. Liu^{1,a}, Zhiqiang Liu¹, Zhiqing Liu²², H. Loehner²⁵, X. C. Lou^{1,a,h}, H. J. Lu¹⁷, J. G. Lu^{1,a}, R. Q. Lu¹⁸, Y. Lu¹, Y. P. Lu^{1,a}, C. L. Luo²⁸, M. X. Luo⁵¹, T. Luo⁴², X. L. Luo^{1,a}, M. Lv¹, X. R. Lyu⁴¹, F. C. Ma²⁷, H. L. Ma¹, L. L. Ma³³, Q. M. Ma¹, T. Ma¹, X. N. Ma³⁰, X. Y. Ma^{1,a}, F. E. Maas¹⁴, M. Maggiora^{48A,48C}, Y. J. Mao³¹, Z. P. Mao¹, S. Marcello^{48A,48C}, J. G. Messchendorp²⁵, J. Min^{1,a}, T. J. Min¹, R. E. Mitchell¹⁹, X. H. Mo^{1,a}, Y. J. Mo⁶, C. Morales Morales¹⁴, K. Moriya¹⁹, N. Yu. Muchnoi^{9,f}, H. Muramatsu⁴³, Y. Nefedov²³, F. Nerling¹⁴, I. B. Nikolaev^{9,f}, Z. Ning^{1,a}, S. Nisar⁸, S. L. Niu^{1,a}, X. Y. Niu¹, S. L. Olsen³², Q. Ouyang^{1,a}, S. Pacetti^{20B}, P. Patteri^{20A}, M. Pelizaeus⁴, H. P. Peng^{45,a}, K. Peters¹⁰, J. Pettersson⁴⁹, J. L. Ping²⁸, R. G. Ping¹, R. Poling⁴³, V. Prasad¹, Y. N. Pu¹⁸, M. Qi²⁹, S. Qian^{1,a}, C. F. Qiao⁴¹, L. Q. Qin³³, N. Qin⁵⁰, X. S. Qin¹, Y. Qin³¹, Z. H. Qin^{1,a}, J. F. Qiu¹, K. H. Rashid⁴⁷, C. F. Redmer²², H. L. Ren¹⁸, M. Ripka²², G. Rong¹, Ch. Rosner¹⁴, X. D. Ruan¹², V. Santoro^{21A}, A. Sarantsev^{23,g}, M. Savrić^{21B}, K. Schoenning⁴⁹, S. Schumann²², W. Shan³¹, M. Shao^{45,a}, C. P. Shen², P. X. Shen³⁰, X. Y. Shen¹, H. Y. Sheng¹, W. M. Song¹, X. Y. Song¹, S. Sosio^{48A,48C}, S. Spataro^{48A,48C}, G. X. Sun¹, J. F. Sun¹⁵, S. S. Sun¹, Y. J. Sun^{45,a}, Y. Z. Sun¹, Z. J. Sun^{1,a}, Z. T. Sun¹⁹, C. J. Tang³⁶, X. Tang¹, I. Tapan^{40C}, E. H. Thorndike⁴⁴, M. Tiemens²⁵, M. Ullrich²⁴, I. Uman^{40B}, G. S. Varner⁴², B. Wang³⁰, B. L. Wang⁴¹, D. Wang³¹, D. Y. Wang³¹, K. Wang^{1,a}, L. L. Wang¹, L. S. Wang¹, M. Wang³³, P. Wang¹, P. L. Wang¹, S. G. Wang³¹, W. Wang^{1,a}, X. F. Wang³⁹, Y. D. Wang¹⁴, Y. F. Wang^{1,a}, Y. Q. Wang²², Z. Wang^{1,a}, Z. G. Wang^{1,a}, Z. H. Wang^{45,a}, Z. Y. Wang¹, T. Weber²², D. H. Wei¹¹, J. B. Wei³¹, P. Weidenkaff²², S. P. Wen¹, U. Wiedner⁴, M. Wolke⁴⁹, L. H. Wu¹, Z. Wu^{1,a}, L. G. Xia³⁹, Y. Xia¹⁸, D. Xiao¹, Z. J. Xiao²⁸, Y. G. Xie^{1,a}, Q. L. Xiu^{1,a}, G. F. Xu¹, L. Xu¹, Q. J. Xu¹³, Q. N. Xu⁴¹, X. P. Xu³⁷, L. Yan^{45,a}, W. B. Yan^{45,a}, W. C. Yan^{45,a}, Y. H. Yan¹⁸, H. J. Yang³⁴, H. X. Yang¹, L. Yang⁵⁰, Y. Yang⁶, Y. X. Yang¹¹, H. Ye¹, M. Ye^{1,a}, M. H. Ye⁷, J. H. Yin¹, B. X. Yu^{1,a}, C. X. Yu³⁰, H. W. Yu³¹, J. S. Yu²⁶, C. Z. Yuan¹, W. L. Yuan²⁹, Y. Yuan¹, A. Yuncu^{40B,c}, A. A. Zafar⁴⁷, A. Zallo^{20A}, Y. Zeng¹⁸, B. X. Zhang¹, B. Y. Zhang^{1,a}, C. Zhang²⁹, C. C. Zhang¹, D. H. Zhang¹, H. H. Zhang³⁸, H. Y. Zhang^{1,a}, J. J. Zhang¹, J. L. Zhang¹, J. Q. Zhang¹, J. W. Zhang^{1,a}, J. Y. Zhang¹, J. Z. Zhang¹, K. Zhang¹, L. Zhang¹, S. H. Zhang¹, X. Y. Zhang³³, Y. Zhang¹, Y. N. Zhang⁴¹, Y. H. Zhang^{1,a}, Y. T. Zhang^{45,a}, Yu Zhang⁴¹, Z. H. Zhang⁶, Z. P. Zhang⁴⁵, Z. Y. Zhang⁵⁰, G. Zhao¹, J. W. Zhao^{1,a}, J. Y. Zhao¹, J. Z. Zhao^{1,a}, Lei Zhao^{45,a}, Ling Zhao¹, M. G. Zhao³⁰, Q. Zhao¹, Q. W. Zhao¹, S. J. Zhao⁵², T. C. Zhao¹, Y. B. Zhao^{1,a}, Z. G. Zhao^{45,a}, A. Zhemchugov^{23,d}, B. Zheng⁴⁶, J. P. Zheng^{1,a}, W. J. Zheng³³, Y. H. Zheng⁴¹, B. Zhong²⁸, L. Zhou^{1,a}, Li Zhou³⁰, X. Zhou⁵⁰, X. K. Zhou^{45,a}, X. R. Zhou^{45,a}, X. Y. Zhou¹, K. Zhu¹, K. J. Zhu^{1,a}, S. Zhu¹, X. L. Zhu³⁹, Y. C. Zhu^{45,a}, Y. S. Zhu¹, Z. A. Zhu¹, J. Zhuang^{1,a}, L. Zotti^{48A,48C}, B. S. Zou¹, J. H. Zou¹

(BESIII Collaboration)

¹ Institute of High Energy Physics, Beijing 100049, People's Republic of China

² Beihang University, Beijing 100191, People's Republic of China

³ Beijing Institute of Petrochemical Technology, Beijing 102617, People's Republic of China

⁴ Bochum Ruhr-University, D-44780 Bochum, Germany

⁵ Carnegie Mellon University, Pittsburgh, Pennsylvania 15213, USA

⁶ Central China Normal University, Wuhan 430079, People's Republic of China

⁷ China Center of Advanced Science and Technology, Beijing 100190, People's Republic of China

⁸ COMSATS Institute of Information Technology, Lahore, Defence Road, Off Raiwind Road, 54000 Lahore, Pakistan

⁹ G.I. Budker Institute of Nuclear Physics SB RAS (BINP), Novosibirsk 630090, Russia

¹⁰ GSI Helmholtzcentre for Heavy Ion Research GmbH, D-64291 Darmstadt, Germany

¹¹ Guangxi Normal University, Guilin 541004, People's Republic of China

¹² GuangXi University, Nanning 530004, People's Republic of China

- ¹³ Hangzhou Normal University, Hangzhou 310036, People's Republic of China
- ¹⁴ Helmholtz Institute Mainz, Johann-Joachim-Becher-Weg 45, D-55099 Mainz, Germany
- ¹⁵ Henan Normal University, Xinxiang 453007, People's Republic of China
- ¹⁶ Henan University of Science and Technology, Luoyang 471003, People's Republic of China
- ¹⁷ Huangshan College, Huangshan 245000, People's Republic of China
- ¹⁸ Hunan University, Changsha 410082, People's Republic of China
- ¹⁹ Indiana University, Bloomington, Indiana 47405, USA
- ²⁰ (A)INFN Laboratori Nazionali di Frascati, I-00044, Frascati, Italy; (B)INFN and University of Perugia, I-06100, Perugia, Italy
- ²¹ (A)INFN Sezione di Ferrara, I-44122, Ferrara, Italy; (B)University of Ferrara, I-44122, Ferrara, Italy
- ²² Johannes Gutenberg University of Mainz, Johann-Joachim-Becher-Weg 45, D-55099 Mainz, Germany
- ²³ Joint Institute for Nuclear Research, 141980 Dubna, Moscow region, Russia
- ²⁴ Justus Liebig University Giessen, II. Physikalisches Institut, Heinrich-Buff-Ring 16, D-35392 Giessen, Germany
- ²⁵ KVI-CART, University of Groningen, NL-9747 AA Groningen, The Netherlands
- ²⁶ Lanzhou University, Lanzhou 730000, People's Republic of China
- ²⁷ Liaoning University, Shenyang 110036, People's Republic of China
- ²⁸ Nanjing Normal University, Nanjing 210023, People's Republic of China
- ²⁹ Nanjing University, Nanjing 210093, People's Republic of China
- ³⁰ Nankai University, Tianjin 300071, People's Republic of China
- ³¹ Peking University, Beijing 100871, People's Republic of China
- ³² Seoul National University, Seoul, 151-747 Korea
- ³³ Shandong University, Jinan 250100, People's Republic of China
- ³⁴ Shanghai Jiao Tong University, Shanghai 200240, People's Republic of China
- ³⁵ Shanxi University, Taiyuan 030006, People's Republic of China
- ³⁶ Sichuan University, Chengdu 610064, People's Republic of China
- ³⁷ Soochow University, Suzhou 215006, People's Republic of China
- ³⁸ Sun Yat-Sen University, Guangzhou 510275, People's Republic of China
- ³⁹ Tsinghua University, Beijing 100084, People's Republic of China
- ⁴⁰ (A)Istanbul Aydin University, 34295 Sefakoy, Istanbul, Turkey; (B)Dogus University, 34722 Istanbul, Turkey; (C)Uludag University, 16059 Bursa, Turkey
- ⁴¹ University of Chinese Academy of Sciences, Beijing 100049, People's Republic of China
- ⁴² University of Hawaii, Honolulu, Hawaii 96822, USA
- ⁴³ University of Minnesota, Minneapolis, Minnesota 55455, USA
- ⁴⁴ University of Rochester, Rochester, New York 14627, USA
- ⁴⁵ University of Science and Technology of China, Hefei 230026, People's Republic of China
- ⁴⁶ University of South China, Hengyang 421001, People's Republic of China
- ⁴⁷ University of the Punjab, Lahore-54590, Pakistan
- ⁴⁸ (A)University of Turin, I-10125, Turin, Italy; (B)University of Eastern Piedmont, I-15121, Alessandria, Italy; (C)INFN, I-10125, Turin, Italy
- ⁴⁹ Uppsala University, Box 516, SE-75120 Uppsala, Sweden
- ⁵⁰ Wuhan University, Wuhan 430072, People's Republic of China
- ⁵¹ Zhejiang University, Hangzhou 310027, People's Republic of China
- ⁵² Zhengzhou University, Zhengzhou 450001, People's Republic of China
- ^a Also at State Key Laboratory of Particle Detection and Electronics, Beijing 100049, Hefei 230026, People's Republic of China
- ^b Also at Ankara University, 06100 Tandogan, Ankara, Turkey
- ^c Also at Bogazici University, 34342 Istanbul, Turkey
- ^d Also at the Moscow Institute of Physics and Technology, Moscow 141700, Russia
- ^e Also at the Functional Electronics Laboratory, Tomsk State University, Tomsk, 634050, Russia
- ^f Also at the Novosibirsk State University, Novosibirsk, 630090, Russia
- ^g Also at the NRC "Kurchatov Institute, PNPI, 188300, Gatchina, Russia
- ^h Also at University of Texas at Dallas, Richardson, Texas 75083, USA
- ⁱ Currently at Istanbul Arel University, 34295 Istanbul, Turkey

The decay $Z_c(3900)^\pm \rightarrow \omega\pi^\pm$ is searched for using data samples collected with the BESIII detector operating at the BEPCII storage ring at center-of-mass energies $\sqrt{s} = 4.23$ and 4.26 GeV. No significant signal for the $Z_c(3900)^\pm$ is found, and upper limits at the 90% confidence level on the Born cross section for the process $e^+e^- \rightarrow Z_c(3900)^\pm\pi^\mp \rightarrow \omega\pi^+\pi^-$ are determined to be 0.26 and 0.18 pb at $\sqrt{s} = 4.23$ and 4.26 GeV, respectively.

I. INTRODUCTION

Recently, in the study of $e^+e^- \rightarrow J/\psi\pi^+\pi^-$, a distinct charged structure, named the $Z_c(3900)^\pm$, was observed in the $J/\psi\pi^\pm$ spectrum by BESIII [1] and Belle [2]. Its existence was confirmed shortly thereafter with CLEO-c data [3]. The existence of the neutral partner in the decay $Z_c(3900)^0 \rightarrow J/\psi\pi^0$ has also been reported in CLEO-c data [3] and by BESIII [4]. The $Z_c(3900)$ is a good candidate for an exotic state beyond simple quark models, since it contains a $c\bar{c}$ pair and is also electrically charged. Noting that the $Z_c(3900)$ has a mass very close to the $D^*\bar{D}$ threshold (3875 MeV), BESIII analyzed the process $e^+e^- \rightarrow \pi^\pm(D\bar{D}^*)^\mp$, and a clear structure in the $(D\bar{D}^*)^\mp$ mass spectrum is seen, called the $Z_c(3885)$. The measured mass and width are $(3883.9 \pm 1.5 \pm 4.2)$ MeV/ c^2 and $(24.8 \pm 3.3 \pm 11.0)$ MeV, respectively, and quantum numbers $J^P = 1^+$ are favored [5]. Assuming the $Z_c(3885) \rightarrow D\bar{D}^*$ and the $Z_c(3900) \rightarrow J/\psi\pi$ signals are from the same source, the ratio of partial widths $\frac{\Gamma(Z_c(3885) \rightarrow D\bar{D}^*)}{\Gamma(Z_c(3900) \rightarrow J/\psi\pi)}$ is determined to be $6.2 \pm 1.1 \pm 2.7$.

The observation of the $Z_c(3900)$ has stimulated many theoretical studies of its nature. Possible interpretations are tetra-quark [6], hadro-charmonium [7], $D^*\bar{D}$ molecule [8] and threshold effects [9–11]. Lattice QCD studies provide theoretical support for the existence of $X(3872)$ [12] but not for the $Z_c(3900)$ [13–17]. However, those studies were carried out on small volumes with unphysically heavy up and down quarks. It is also worth noting that no resonant structure in $J/\psi\pi$ is observed in $\bar{B}^0 \rightarrow J/\psi\pi^+\pi^-$ by LHCb [18], in $\bar{B}^0 \rightarrow J/\psi K^-\pi^+$ by Belle [19] or in $\gamma p \rightarrow J/\psi\pi^+n$ by COMPASS [20].

The decay properties of a state can provide useful information on its internal structure. There are three important decay modes for charmonium-like states: (i) “fall-apart” decays to open charm mesons; (ii) cascades to hidden charm mesons; and (iii) decays to light hadrons via intermediate gluons. In addition, as shown in Ref. [9, 10], an enhancement near the $D\bar{D}^*$ threshold can be produced via rescattering of hidden or open charm final states. Decays of the $Z_c(3900)$ to light hadrons can play a unique role in distinguishing a resonance from threshold effects, because the decay mode with $c\bar{c}$ annihilation involves neither hidden nor open charm final states. However, theory estimates of annihilation widths to light hadrons are only order of magnitude due to uncertainties of wave function effects and QCD corrections [21, 22]. A sizeable $Z_c(3900)$ decay width to light hadrons might be expected in analogy to η_c or χ_{cJ} into hadronic final states.

Among a large number of hadronic final states that are available for a $I^G(J^P) = 1^+(1^+)$ resonance decay, $\omega\pi$ is one of the typical decay modes which are not suppressed by any known selection rule. In this paper, we report a search for $Z_c(3900)^\pm \rightarrow \omega\pi^\pm$ based on e^+e^- annihilation

samples taken at center-of-mass (CM) energies $\sqrt{s} = 4.23$ and 4.26 GeV. The data samples were collected with the BESIII [23] detector operating at the BEPCII storage ring. The integrated luminosity of these data samples are measured by analyzing the large-angle Bhabha scattering events with an uncertainty of 1.0% [24] and are equal to 1092 pb $^{-1}$ and 826 pb $^{-1}$, for $\sqrt{s} = 4.23$ and 4.26 GeV, respectively.

II. BESIII EXPERIMENT AND MONTE CARLO SIMULATION

The BESIII detector, described in detail in Ref. [23], has a geometrical acceptance of 93% of 4π . A small-cell helium-based main drift chamber (MDC) provides a charged particle momentum resolution of 0.5% at 1 GeV/ c in a 1 T magnetic field, and supplies energy-loss (dE/dx) measurements with a resolution of 6% for minimum-ionizing pions. The electromagnetic calorimeter (EMC) measures photon energies with a resolution of 2.5% (5%) at 1.0 GeV in the barrel (end-caps). Particle identification (PID) is provided by a time-of-flight system (TOF) with a time resolution of 80 ps (110 ps) for the barrel (end-caps). The muon system, located in the iron flux return yoke of the magnet, provides 2 cm position resolution and detects muon tracks with momenta greater than 0.5 GeV/ c .

The GEANT4-based [25] Monte Carlo (MC) simulation software BOOST [26] includes the geometric description of the BESIII detector and a simulation of the detector response. It is used to optimize event selection criteria, estimate backgrounds and evaluate the detection efficiency. We generate signal MC samples of $e^+e^- \rightarrow Z_c(3900)^\pm\pi^\mp \rightarrow \omega\pi^+\pi^-$ uniformly in phase space, where the ω decays to $\pi^+\pi^-\pi^0$. The decays of $\omega \rightarrow \pi^+\pi^-\pi^0$ are generated with the *OMEGA_DALITZ* model in EVTGEN [27, 28]. Initial state radiation (ISR) is simulated with KKMC [29, 30], where the Born cross section of $e^+e^- \rightarrow Z_c(3900)^\pm\pi^\mp$ is assumed to follow a $Y(4260)$ Breit-Wigner (BW) line shape with resonance parameters taken from the Particle Data Group (PDG) [31]. Final state radiation (FSR) effects associated with charged particles are handled with PHOTOS [29]. For studies of possible backgrounds, inclusive $Y(4260)$ MC samples with luminosity equivalent to the experimental data at $\sqrt{s} = 4.23$ and $\sqrt{s} = 4.26$ GeV are generated, where the main known decay channels are generated using EVTGEN [27, 28] with branching fractions taken from the PDG [31]. The remaining events associated with charmonium decays are generated with LUNDCHARM [32], while continuum hadronic events are generated with PYTHIA [33]. QED processes such as Bhabha scattering, dimuon and digamma events are generated with KKMC [29, 30].

III. DATA ANALYSIS AND BACKGROUND STUDY

Tracks of charged particles in BESIII are reconstructed from MDC hits. We select tracks with their point of closest approach within ± 10 cm of the interaction point in the beam direction and within 1 cm in the plane perpendicular to the beam. Information from the TOF and dE/dx measurements are combined to form PID confidence levels for the π and K hypotheses; each track is assigned to the particle type with the highest confidence level.

Photon candidates are reconstructed by clustering EMC crystal energies. The efficiency and energy resolution are improved by including energy deposits in nearby TOF counters. The minimum energy is required to be 25 MeV for barrel showers ($|\cos\theta| < 0.80$) and 50 MeV for endcap showers ($0.86 < |\cos\theta| < 0.92$). To exclude showers from charged particles, the angle between the shower and the extrapolated charged tracks at the EMC must be greater than 5° . A requirement on the EMC cluster timing with respect to the event start time is applied to suppress electronic noise and energy deposits unrelated to the event.

The π^0 candidates are formed from pairs of photons that can be kinematically fitted to the known π^0 mass. The χ^2 from this fit with one degree of freedom is required to be less than 25.

Events with exactly four charged tracks identified as pions with zero net charge and at least one π^0 candidate are selected. A five-constraint kinematic fit (5C) is performed to the hypothesis of $e^+e^- \rightarrow \pi^+\pi^-\pi^+\pi^-\pi^0$ (constraints are the 4-momentum of the initial e^+e^- system and the π^0 mass), and $\chi_{5C}^2 < 40$ is required. If there more than one π^0 is found in an event, the combination with the smallest χ_{5C}^2 is retained.

Figure 1 shows the $\pi^+\pi^-\pi^0$ invariant mass distribution of the $\pi^+\pi^-\pi^0$ combination with invariant mass closest to the mass of ω for the selected candidate $e^+e^- \rightarrow \pi^+\pi^-\pi^+\pi^-\pi^0$ events at $\sqrt{s} = 4.23$ GeV, where prominent η , ω and ϕ signals are observed.

ω candidates are selected with the mass window $|M(\pi^+\pi^-\pi^0)_{\text{closest}} - m_\omega| < 0.03$ GeV/ c^2 , where m_ω is the nominal mass of the ω taken from the PDG [31]. Figure 2 shows the $M(\omega\pi^\pm)$ distribution for the candidate events of $e^+e^- \rightarrow \omega\pi^+\pi^-$ at $\sqrt{s} = 4.23$ GeV. No sign of a peak near 3.9 GeV/ c^2 is apparent. The shaded histogram in Fig. 2 shows the distribution of non- ω background for the events in ω sideband regions ($0.06 < |M(\pi^+\pi^-\pi^0)_{\text{closest}} - m_\omega| < 0.09$ GeV/ c^2).

By studying inclusive MC samples with luminosity equivalent to the data at $\sqrt{s} = 4.23$ and 4.26 GeV, the background is found to be dominantly from the continuum process $e^+e^- \rightarrow \omega\pi^+\pi^-$. The solid histogram in Fig. 2 shows the $\omega\pi^\pm$ invariant mass distribution for events selected from the inclusive MC sample.

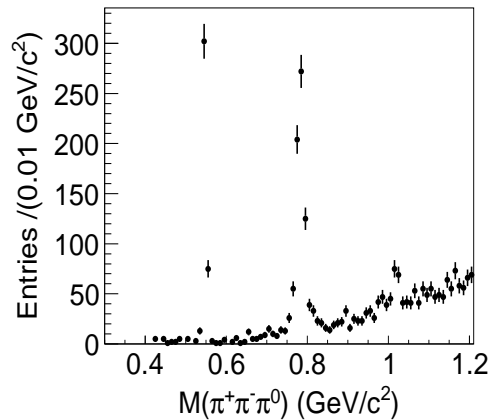


FIG. 1. The $\pi^+\pi^-\pi^0$ invariant mass distribution of the combination closest to the ω , for the selected $e^+e^- \rightarrow \pi^+\pi^-\pi^+\pi^-\pi^0$ candidates for the data sample at $\sqrt{s} = 4.23$ GeV.

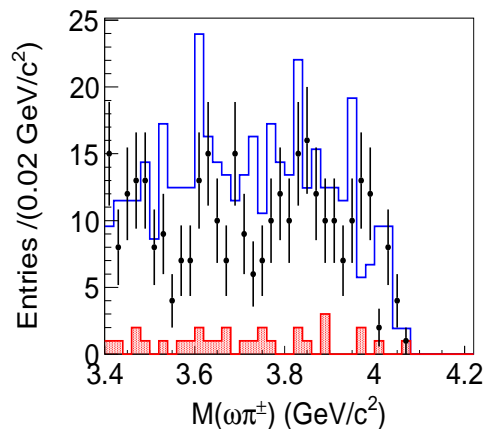


FIG. 2. Distribution of $M(\omega\pi^\pm)$ for the data sample at $\sqrt{s} = 4.23$ GeV. The dots with error bars are events within the ω signal region. The shaded histogram shows events selected from the ω sidebands, and the solid histogram shows inclusive MC events, which are dominated by continuum events.

IV. FITTING RESULTS

We use a one-dimensional, unbinned, extended maximum likelihood fit to the $\omega\pi^\pm$ invariant mass distribution to obtain the yield of $Z_c(3900)^\pm \rightarrow \omega\pi^\pm$ events. The signal probability density function (PDF) is parameterized by an S -wave Breit-Wigner function convolved with a Gaussian resolution function and weighted with the detection efficiency:

$$\left(G(M; \sigma) \otimes \frac{p \cdot q}{(M^2 - M_0^2)^2 + M_0^2 \Gamma^2} \right) \times \varepsilon(M), \quad (1)$$

where $G(M; \sigma)$ is a Gaussian function representing the mass resolution. The mass resolution of the $Z_c(3900)^\pm$ is 1.2 ± 0.1 MeV/ c^2 at both $\sqrt{s} = 4.23$ and 4.26 GeV,

according to MC simulation. $p \cdot q$ is the S -wave phase space factor, where p is the $Z_c(3900)^\pm$ momentum in the e^+e^- CM frame and q is the ω momentum in the $Z_c(3900)^\pm$ CM frame. M is the invariant mass of $\omega\pi^\pm$, and M_0 and Γ are the mass and width of the $Z_c(3900)^\pm$, which are fixed to the results in Ref [1]. $\epsilon(M)$ is the efficiency curve as a function of the $\omega\pi^\pm$ invariant mass, obtained from signal MC simulation.

The background shape is described by an ARGUS function $M\sqrt{1-(M/m_0)^2} \cdot \exp(c(1-(M/m_0)^2))$, where c is left free in the fit and m_0 is fixed to the threshold of $\sqrt{s} - m_\pi$ [34].

Figure 3(a) shows the fit result for the data sample at $\sqrt{s} = 4.23$ GeV. The fit yields 14 ± 11 events for the $Z_c(3900)^\pm$ signal. Compared to the fit without the $Z_c(3900)^\pm$ signal, the change in $\ln L$ with $\Delta(d.o.f.) = 1$ is 0.74, corresponding to a statistical significance of 1.2σ . Using the Bayesian method [31, Sect.38.4.1], the upper limit for the $Z_c(3900)^\pm$ signal is set to 33.5 events at the 90% confidence level (C.L.), where only the statistical uncertainty is considered.

The fit result for the data sample at $\sqrt{s} = 4.26$ GeV is shown in Fig. 3(b). The fit yields 2.2 ± 8.1 events for the $Z_c(3900)^\pm$ with a statistical significance of 0.1σ . The upper limit is 18.8 events at the 90% C.L.

V. CROSS SECTION UPPER LIMITS AND SYSTEMATIC UNCERTAINTY

The upper limit on the Born cross section at the 90% C.L. is calculated as

$$\sigma(e^+e^- \rightarrow Z_c(3900)^\pm\pi^\mp, Z_c(3900)^\pm \rightarrow \omega\pi^\pm) = \frac{N^{\text{UL}}}{\mathcal{L}_{\text{int}}(1+\delta)\frac{1}{|1-\Pi|^2}\epsilon(1-\sigma_\epsilon)\mathcal{B}_\omega\mathcal{B}_{\pi^0}}, \quad (2)$$

where N^{UL} is the upper limit on the signal events; \mathcal{L}_{int} is the integrated luminosity; ϵ is the selection efficiency obtained from signal MC simulation, which are $18.5 \pm 0.2\%$ and $18.6 \pm 0.2\%$ at $\sqrt{s} = 4.23$ and 4.26 GeV, respectively; σ_ϵ is the systematic uncertainty of the efficiency described in next paragraph; $\frac{1}{|1-\Pi|^2}$ is the vacuum polarization factor obtained by using calculations from Ref. [35], and equal to 1.06 for both energies; $(1+\delta)$ is the radiative correction factor, equal to 0.844 for $\sqrt{s} = 4.23$ GeV and 0.848 for $\sqrt{s} = 4.26$ GeV obtained using Ref. [29, 30] by assuming the line shape of Born cross section $\sigma(e^+e^- \rightarrow Z_c(3900)^\pm\pi^\mp)$ to be a BW function with the parameters of the $Y(4260)$ taken from PDG [31]; and \mathcal{B}_ω and \mathcal{B}_{π^0} are the branching fractions of the decay $\omega \rightarrow \pi^+\pi^-\pi^0$ and $\pi^0 \rightarrow \gamma\gamma$ [31], respectively. A conservative estimate of the upper limit of the Born cross section is determined by lowering the efficiency by one standard deviation of the systematic uncertainty.

The systematic uncertainty of the cross section measurement from Eq. 2 is summarized in Table I. The luminosity is measured using Bhabha events with an un-

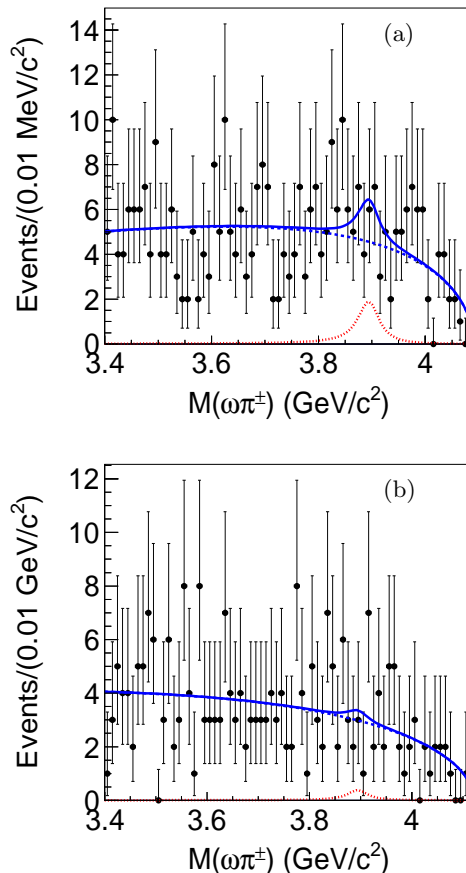


FIG. 3. Results of the unbinned maximum likelihood fit of the $\omega\pi^\pm$ mass spectrum of $e^+e^- \rightarrow \omega\pi^+\pi^-$ at (a) $\sqrt{s} = 4.23$ GeV and (b) $\sqrt{s} = 4.26$ GeV. Dots with error bars are the data. The solid curve is the result of the fit described in the text. The dotted curve is the $Z_c(3900)^\pm$ signal. The dashed curve is the background.

certainty of 1.0% [24]. The uncertainty in tracking efficiency for pions is 1.0% per track [5], i.e. 4.0% for the track selection in this analysis. The uncertainty in PID efficiency for pions is 1.0% per track [5]. The uncertainty in the photon reconstruction efficiency is less than 1% per photon [36]. The uncertainty in the π^0 reconstruction efficiency is 2.0% [37]. The uncertainty of the kinematic fit is estimated by correcting the helix parameters of the charged tracks. The detailed procedure to extract the correction factors can be found in Ref. [38]. The track parameters in MC samples are corrected by these factors, and the difference in efficiencies of 0.8% with and without the correction is taken as the systematic uncertainty associated with the kinematic fit. An MC sample generated with $Z_c(3900)^\pm \rightarrow \omega\pi^\pm$ in both S wave and D wave, assuming a D/S waves amplitude ratio of 0.1, results in a 3% change in detection efficiency. This difference is taken as the systematic uncertainty associated with the MC production model. The branching ratio value for $\omega \rightarrow \pi^+\pi^-\pi^0$ comes from the PDG [31], and its error is

TABLE I. Summary of the relative systematic uncertainties of the cross section measurement (in %).

Source	$\sqrt{s} = 4.23$ GeV	$\sqrt{s} = 4.26$ GeV
Luminosity	1.0	1.0
Tracking	4.0	4.0
PID	4.0	4.0
photon reconstruction	2.0	2.0
π^0 reconstruction	2.0	2.0
Kinematic fit	0.8	0.8
Decay model	3	3
Radiative correction	6	7
$Br(\omega \rightarrow \pi^+\pi^-\pi^0)$	0.8	0.8
Total	9.4	10.1

0.8%. In the nominal fit, the radiative correction factor and the detection efficiency are determined under the assumption that the production of $e^+e^- \rightarrow Z_c(3900)^\pm\pi^\mp$ follows the $Y(4260)$ line shape. Using the line shape of $\sigma(e^+e^- \rightarrow Z_c(3900)^0\pi^0)$ measured in Ref. [4] as an alternative assumption, $\epsilon(1+\delta)$ is increased by 6% for $\sqrt{s} = 4.23$ GeV and 7% for $\sqrt{s} = 4.26$ GeV. The change in $\epsilon(1+\delta)$ is taken as a systematic uncertainty. The uncertainty of the vacuum polarization factor is taken from Ref. [35], and is negligible compared with other uncertainties. Assuming that all sources of systematic uncertainties are independent, the total errors are given by the quadratic sums.

To estimate the systematic uncertainties due to the fit procedure, we fit under different scenarios, and the upper limits obtained at the 90% C.L. for the $Z_c(3900)^\pm$ signal yield are summarized in Table II. The effect on the signal yield from the fit range is obtained by varying the fit range by ± 0.1 GeV/ c^2 . The effect due to the choice of the background shape is estimated by changing the background shape from the ARGUS function to a second order polynomial (where the parameters of the polynomial are allowed to vary and the fit range is limited to [3.4, 4.08] GeV/ c^2). The effect due to the resonance parameters of the $Z_c(3900)^\pm$ is estimated by varying the resonance parameters according to the results in Ref [5]. The effect due to the mass resolution is estimated by increasing the resolution by 10% according to the comparison between the data and MC. The effect due to the mass-dependent efficiency curve is estimated by changing the efficiency curve to a constant function. We take the largest number of $Z_c(3900)^\pm$ events in the different scenarios as a conservative estimate of the upper limit: $N_{4230}^{\text{UL}} = 38.0$, $N_{4260}^{\text{UL}} = 18.8$. The resulting upper limits of the Born cross sections at $\sqrt{s} = 4.23$ and 4.26 GeV are determined to be 0.26 and 0.18 pb at the 90% C.L., respectively.

VI. SUMMARY AND DISCUSSION

In summary, based on data samples of 1092 pb $^{-1}$ at $\sqrt{s} = 4.23$ GeV and 826 pb $^{-1}$ at $\sqrt{s} = 4.26$ GeV

TABLE II. Results of upper limits on the $Z_c(3900)$ signal yield with various fit procedures.

Source	$\sqrt{s} = 4.23$ GeV	$\sqrt{s} = 4.26$ GeV
Fit range	31.5	18.5
Background shape	38.0	16.1
$Z_c(3900)$ mass and width	22.6	12.2
Mass resolution	33.5	18.8
Efficiency curve	33.3	18.8

collected with the BESIII detector operating at the BEPCII storage ring, a search is performed for the decay $Z_c(3900)^\pm \rightarrow \omega\pi^\pm$ in $e^+e^- \rightarrow \omega\pi^+\pi^-$. No $Z_c(3900)^\pm$ signal is observed. The corresponding upper limits on the Born cross section are set to be 0.26 and 0.18 pb at $\sqrt{s} = 4.23$ and 4.26 GeV, respectively. If we assume that the $Z_c(3900)^\pm$ observed in $e^+e^- \rightarrow J/\psi\pi^+\pi^-$ [1] and $Z_c(3885)^\pm$ in $e^+e^- \rightarrow (D\bar{D}^*)^\pm\pi^\mp$ [5] are the same particle, the decay width of $Z_c(3900)^\pm \rightarrow \omega\pi^\pm$ is estimated to be smaller than 0.2% of the $Z_c(3900)^\pm$ total width. As $\omega\pi$ is a typical light hadron decay mode of a $I^G(J^P) = 1^+(1^+)$ resonance, the non-observation of $Z_c(3900)^\pm \rightarrow \omega\pi^\pm$ may indicate that the annihilation of $c\bar{c}$ in $Z_c(3900)^\pm$ is suppressed. Complementary to the searches for $Z_c(3900)$ production [18–20], exploring new $Z_c(3900)$ decay modes may provide a significant input to clarify its dynamical origin.

ACKNOWLEDGMENTS

The BESIII collaboration thanks the staff of BEPCII and the IHEP computing center for their strong support. This work is supported in part by National Key Basic Research Program of China under Contract No. 2015CB856700; National Natural Science Foundation of China (NSFC) under Contracts Nos. 11125525, 11235011, 11322544, 11335008, 11425524; the Chinese Academy of Sciences (CAS) Large-Scale Scientific Facility Program; Joint Large-Scale Scientific Facility Funds of the NSFC and CAS under Contracts Nos. 11179007, U1232201, U1332201; CAS under Contracts Nos. KJCX2-YW-N29, KJCX2-YW-N45; 100 Talents Program of CAS; INPAC and Shanghai Key Laboratory for Particle Physics and Cosmology; German Research Foundation DFG under Contract No. Collaborative Research Center CRC-1044; Istituto Nazionale di Fisica Nucleare, Italy; Ministry of Development of Turkey under Contract No. DPT2006K-120470; Russian Foundation for Basic Research under Contract No. 14-07-91152; U. S. Department of Energy under Contracts Nos. DE-FG02-04ER41291, DE-FG02-05ER41374, DE-FG02-94ER40823, DESC0010118; U.S. National Science Foundation; University of Groningen (RuG) and the Helmholtzzentrum fuer Schwerionenforschung GmbH (GSI), Darmstadt; WCU Program of National Research Foundation of Korea under Contract No. R32-2008-000-

-
- [1] M. Ablikim *et al.* [BESIII Collaboration], Phys. Rev. Lett. **110**, 252001 (2013)
- [2] Z. Q. Liu *et al.* [Belle Collaboration], Phys. Rev. Lett. **110**, 252002 (2013)
- [3] T. Xiao, S. Dobbs, A. Tomaradze and K. K. Seth, Phys. Lett. B **727**, 366 (2013)
- [4] M. Ablikim *et al.* [BESIII Collaboration], arXiv:1506.06018 [hep-ex].
- [5] M. Ablikim *et al.* [BESIII Collaboration], Phys. Rev. Lett. **112**, 022001 (2014)
- [6] L. Maiani, V. Riquer, R. Faccini, F. Piccinini, A. Pilloni and A. D. Polosa, Phys. Rev. D **87**, 111102 (2013)
- [7] M. B. Voloshin, Phys. Rev. D **87**, 091501 (2013)
- [8] F. -K. Guo, C. Hidalgo-Duque, J. Nieves and M. P. Valderrama, Phys. Rev. D **88**, 054007 (2013)
- [9] Q. Wang, C. Hanhart and Q. Zhao, Phys. Rev. Lett. **111**, 132003 (2013)
- [10] D. -Y. Chen, X. Liu and T. Matsuki, Phys. Rev. Lett. **110**, 232001 (2013)
- [11] E. S. Swanson, Phys. Rev. D **91**, 034009 (2015)
- [12] S. Prelovsek and L. Leskovec, Phys. Rev. Lett. **111**, 192001 (2013)
- [13] S. Prelovsek and L. Leskovec, Phys. Lett. B **727**, 172 (2013)
- [14] S. Prelovsek, C. B. Lang, L. Leskovec and D. Mohler, Phys. Rev. D **91**, 014504 (2015)
- [15] L. Leskovec, S. Prelovsek, C. B. Lang and D. Mohler, arXiv:1410.8828 [hep-lat].
- [16] S. h. Lee *et al.* [Fermilab Lattice and MILC Collaborations], arXiv:1411.1389 [hep-lat].
- [17] Y. Chen, M. Gong, Y. H. Lei, N. Li, J. Liang, C. Liu, H. Liu and J. L. Liu *et al.*, Phys. Rev. D **89**, 094506 (2014)
- [18] R. Aaij *et al.* [LHCb Collaboration], Phys. Rev. D **90**, 012003 (2014)
- [19] K. Chilikin *et al.* [Belle Collaboration], Phys. Rev. D **90**, 112009 (2014)
- [20] C. Adolph *et al.* [COMPASS Collaboration], Phys. Lett. B **742**, 330 (2015)
- [21] F. E. Close and S. Godfrey, Phys. Lett. B **574**, 210 (2003)
- [22] E. Braaten and M. Kusunoki, Phys. Rev. D **69**, 074005 (2004)
- [23] M. Ablikim *et al.* (BESIII Collaboration), Nucl. Instrum. Meth. A **614**, 345 (2010).
- [24] M. Ablikim *et al.* [BESIII Collaboration], arXiv:1503.03408 [hep-ex].
- [25] S. Agostinelli *et al.* (GEANT4 Collaboration), Nucl. Instrum. Meth. A **506**, 250 (2003).
- [26] Z. Y. Deng *et al.*, HEP & NP **30**, 371 (2006).
- [27] D. J. Lange, Nucl. Instrum. Methods Phys. Res., Sect. A **462**, 152 (2001).
- [28] R. -G. Ping, Chin. Phys. C **32**, 599 (2008).
- [29] S. Jadach, B. F. L. Ward and Z. Was, Comput. Phys. Commun. **130**, 260 (2000).
- [30] S. Jadach, B. F. L. Ward and Z. Was, Phys. Rev. D **63**, 113009 (2001).
- [31] K. A. Olive *et al.* [Particle Data Group Collaboration], Chin. Phys. C **38**, 090001 (2014).
- [32] J. C. Chen, G. S. Huang, X. R. Qi, D. H. Zhang and Y. S. Zhu, Phys. Rev. D **62** 034003 (2000).
- [33] T. Sjostrand, S. Mrenna and P. Z. Skands, JHEP **0605**, 026 (2006)
- [34] H. Albrecht *et al.* [ARGUS Collaboration], Phys. Lett. B **241**, 278 (1990).
- [35] S. Actis *et al.* [Working Group on Radiative Corrections and Monte Carlo Generators for Low Energies Collaboration], Eur. Phys. J. C **66**, 585 (2010)
- [36] M. Ablikim *et al.* [BESIII Collaboration], Phys. Rev. D **81**, 052005 (2010)
- [37] M. Ablikim *et al.* [BESIII Collaboration], Phys. Rev. D **83**, 032003 (2011)
- [38] M. Ablikim *et al.* [BESIII Collaboration], Phys. Rev. D **87**, 012002 (2013)